

# Structure and expression identification of Cherry Valley duck IRF8

Tingting Zhang,<sup>\*,†,1</sup> Xinyu Zhai,<sup>\*,1</sup> Xiuyuan Wang,<sup>\*</sup> Jinchao Wang,<sup>\*</sup> Bin Xing,<sup>\*</sup> Runchun Miao,<sup>\*</sup> Tianxu Li,<sup>\*</sup> Tianqi Hong,<sup>\*</sup> and Liangmeng Wei<sup>\*,†,2</sup>

<sup>\*</sup>*Sino-German Cooperative Research Centre for Zoonosis of Animal Origin of Shandong Province, Shandong Provincial Key Laboratory of Animal Biotechnology and Disease Control and Prevention, Shandong Agricultural University, Shandong Provincial Engineering Technology Research Center of Animal Disease Control and Prevention, College of Animal Science and Veterinary Medicine, Shandong Agricultural University, Tai'an City, Shandong Province 271018, China; and* <sup>†</sup>*Collaborative Innovation Center for the Origin and Control of Emerging Infectious Diseases, College of Basic Medical Sciences, Shandong First Medical University, Tai'an City, Shandong Province 271000, China*

**ABSTRACT** Interferon regulatory factor 8 (**IRF8**) is also known as interferon (**IFN**) consensus sequence binding protein (**ICSBP**), which plays an important role in IFN signal transduction. In this study, we cloned the full-length coding sequence of Cherry Valley duck IRF8 (**duIRF8**) and analyzed its structure. In addition, we tested the distribution of IRF8 in the tissues of healthy Cherry Valley ducks, and the changes in IRF8 expression levels in the tissues after virus infection. The results show that the open reading frame (**ORF**) of IRF8 is 1293 bp, encodes 430 amino acids, and have 3 conserved domains: the N-terminal DBD domain, the C-

terminal IAD domain, and the NLS domain. Besides, from the analysis of the phylogenetic tree, it can be known that the duIRF8 has the highest homology with the *anser cygnoides*, and has less homology with the fish. Analyzing the distribution level of IRF8 in the tissues, it is found that the expression level of IRF8 in the liver of Cherry Valley duck is the highest. However, after infection with duck Tambusu virus, novel duck reovirus, and duck plague virus, the expression of IRF8 in the spleen and brain all showed up-regulation. These data indicate that IRF8 is involved in the host's innate immune response against virus in Cherry Valley duck.

**Key words:** IRF8, Cherry Valley duck, cloning, viral infection, innate immunity

2022 Poultry Science 101:101598

<https://doi.org/10.1016/j.psj.2021.101598>

## INTRODUCTION

In the early stage of viral infection, cells produce a series of inflammatory proteins to control virus growth and limit viral infection (Slifka and Whitton, 2000). As an important inflammatory protein, interferon can not only activate cells, but also inhibit virus replication. It plays a particularly important role in innate immunity. With the development of time, people's research on IFN has become more and more in-depth. IFN is an inducible protein, which is induced by cells that recognize pathogen associated molecule patterns (**PAMPs**). Normal cells generally do not produce IFN spontaneously, but once it is produced, it can not only defend against invading viruses but also interfere with the metabolism of

other viruses. Host cells defend against invading viruses by secreting IFN (Pestka et al., 2004). Interferon regulatory factors (**IRFs**) are a group of nuclear factors, named for their ability to regulate the expression of IFN and interferon-inducible genes (**ISGs**) and control the IFN system. Nine members of the IRF family were found in humans and mice. The first member IRF1 was discovered in 1988 (Miyamoto et al., 1988), and IRF10 was found in chickens (Nehyba et al., 2002). IRF8 belongs to the IRF family and plays an important role in interferon signal transduction. It can regulate cell growth and induce and promote the gene differentiation of macrophages and dendritic cells. It is a key transcriptional regulator for the development and function of the immune system (Eisenbeis et al., 1995; Yanai et al., 2012), and can significantly promote the secretion of inflammatory factors (Chmielewski et al., 2016). In addition, IRF8 is known to be an important transcription factor for the development of B cells in bone marrow. It is highly expressed in B cells, and its high expression can promote B cell apoptosis (Pathak et al., 2013). IRF8 is usually induced by IFN- $\gamma$  in dendritic cells and macrophages

© 2021 The Authors. Published by Elsevier Inc. on behalf of Poultry Science Association Inc. This is an open access article under the CC BY-NC-ND license (<http://creativecommons.org/licenses/by-nc-nd/4.0/>).

Received September 8, 2021.

Accepted November 4, 2021.

<sup>1</sup>Tingting Zhang and Xinyu Zhai equally contributed to this paper.

<sup>2</sup>Corresponding author: [lmwei@sdau.edu.cn](mailto:lmwei@sdau.edu.cn)

([Twum et al., 2019](#)), but whether it acts as an activation or inhibitor of transcription depends on the binding of IRF8's DNA binding site and other specific transcription factor families or IRF family transcription factors ([Tamura et al., 2008](#)). Studies have made it clear that IRF8 plays a key role in the differentiation of myeloid cells and promotes the differentiation of monocytes into granulocytes ([Weaver et al., 2007](#)). It is also a crucial regulator in all aspects of dendritic cells development, differentiation and function ([Park et al., 2005](#)), so it is essential for the establishment of the innate immune response.

Duck Tambusu virus (DTMUV) belongs to the genus *Flavivirus*, which is an enveloped positive-stranded single-stranded RNA virus ([Tang et al., 2012](#)). Since the disease was first reported in eastern China in April 2010, the virus has spread widely among ducks in China, causing significant economic losses to the poultry industry ([Yu et al., 2013](#)). The egg production of diseased ducks is significantly reduced, and the mortality rate reaches 10 to 30%. As the disease progresses, the ducks begin to show neurological symptoms, such as unstable standing and falling. The virus mainly damages the nervous system and ovaries, causing duck nerve symptoms and laying duck hemorrhagic oophoritis ([Yun et al., 2012](#)). Many methods can be used for DTMUV detection, such as histological examination, serological examination, virus isolation and molecular detection, but they are time-consuming. Nowadays, the main detection method of DTMUV is the reverse transcriptase real-time PCR detection method, which has the advantages of sensitivity and efficiency. Primers and probes are selected from the E gene in the conserved region of DTMUV ([Yan et al., 2011a](#)). Novel duck reovirus (NDRV) was isolated in China in 2011 and named NDRV TH11 strain ([Chen et al., 2012b](#)). The virus grew well in DF-1 cells and produced obvious cytopathic changes. NDRV mainly causes high mortality in ducklings, and is characterized by severe hemorrhage and necrosis of liver, spleen and lung. Today, there is no available prevention and treatment for NDRV ([Chen et al., 2012a](#)). Studies have adopted the visual reverse transcription loop-mediated isothermal amplification (RT-LAMP) detection method to detect the gene encoding the major outer capsid protein of the new duck reovirus (NDRV)  $\sigma$ B ([Li et al., 2018](#)). This method is sensitive, specific, fast and simple. The study detected the viral RNA load in the tissues of NDRV-infected duck, and found that the virus titer in the spleen was the highest, followed by the liver ([Li et al., 2016c](#)). Duck plague virus (DPV) is an enveloped double-stranded DNA virus that can cause lesions in many tissues, especially the spleen and bursa of Fabricius. It is worth mentioning that it can invade the central nervous system and replicate rapidly in the brain ([Li et al., 2016a](#)). Infected chickens showed reduced egg production, tissue bleeding, runny nose, and drooping wings. The virus can spread vertically among ducks, reducing reproduction rate and hatching rate ([Burgess and Yuill, 1981](#)). Duck plague is difficult to monitor and control, because the

duck plague virus can remain asymptomatic carrier and can only be detected during the intermittent shedding of the virus ([Hansen et al., 1999](#)).

In recent years, the duck industry in China has developed rapidly, but at the same time, the outbreak of DTMUV, NDRV, DPV, and other viral diseases also caused significant economic losses to the duck industry in China ([Li et al., 2016b](#)). In recent years, most studies on IRFs have focused on mammals. Chickens and fish ([Nice et al., 2015](#)) have also been reported, but there are relatively few reports on waterfowl, and studies on ducks have not yet appeared. In this study, we cloned Cherry Valley Duck IRF8 (**duIRF8**) and analyzed its structure. We tested the distribution of IRF8 in healthy Cherry Valley duck tissues, and tested the change levels of IRF8 in the tissues after 3 virus infections to reveal the role of IRF8 in resisting viral infections.

## MATERIALS AND METHODS

### *Animals and Viral Infection*

Cherry Valley ducks (1-day-old) were purchased from a local duck embryo hatchery and raised in a suitable environment and provided sufficient feed and drinking water for 3 wk before use. Several common diseases in ducks were detected in this study to determine the baseline status of the healthy ducks. Specifically, when the ducks were 20-day-old, hemagglutination inhibition (**HI**) tests was used to detect the antibodies of avian influenza and Newcastle disease, respectively. In addition, the enzyme-linked immunosorbent assays were performed to determine the negative for NDRV, DTMUV and DPV, respectively ([Li et al., 2016b](#)). And all ducks were confirmed to be negative for the above viruses. DTMUV, NDRV and DPV used in this study are all from this laboratory and mentioned in previous studies ([Li et al., 2016a, 2018; Yan et al., 2011b](#)).

One hundred and twenty 3-wk-old ducks were randomly divided into 4 groups, 30 in each group. Three groups of Cherry Valley ducks were injected intramuscularly with DTMUV ( $10^{5.2}$  TCID<sub>50</sub>/mL, 0.4 mL per duck), NDRV ( $10^{4.5}$  TCID<sub>50</sub>/mL, 0.5 mL per duck), and DPV ( $10^{6.5}$  TCID<sub>50</sub>/mL, 0.3 mL per duck), respectively. In the control group, the Cherry Valley duck was injected intramuscularly with the 0.4 mL phosphate buffered saline (**PBS**). Three healthy Cherry Valley ducks were used for IRF8 tissue distribution analysis, and the spleen and brain of virus-infected ducks were collected at 1, 3, and 5 d past infection (dpi) for gene expression determination. At the end of the study, remaining ducks were euthanized by injection of a lethal dose of sodium pentobarbital.

### *RNA Extraction*

Total RNA was extracted from heart, liver, spleen, lung, kidney, brain, cerebellum, brainstem, thymus, pancreas, bursa of fabric, duodenum, jejunum, ileum, cecum, skin, muscle, glandular stomach, muscular

stomach, trachea, and esophagus of Cherry Valley ducks using a Trizol reagent. Three randomly selected ducks from 4 experimental groups were collected from the spleen and brain to extract RNA using the same method at 1, 3, 5 dpi. Reverse transcription of RNA sample to cDNA using HiScript II One-Step RT-PCR kit (R223-01, Vazyme). The concentration of RNA sample was determined by measuring absorbance at 260 nm, and its quality was verified by its A260/A280 ratio.

### Cloning of duIRF8

DuIRF8 primers were designed with the National Center for Biotechnology Information (NCBI) primer design software (Table 1). The remaining part of duIRF8 sequence was obtained by cloning using Rapid Taq Master Mix (P222, Vazyme). PCR was performed on the cDNA, using gene-specific primers. Products were visualized on 1% agarose gels and purified by using the agarose gel DNA fragment recovery kit (TIANGEN, Beijing, China). PCR was performed under the following conditions: initial denaturation at 95°C for 3 min was followed by 95°C for 15 s; 60°C for 15 s; 72°C for 15 s for 35 cycles with a 5 min final extension at 72°C. The purified PCR product was then sent to the Beijing Jinweizhi Biotechnology Co., Ltd, (Beijing, China) for DNA sequencing. Sequence was analyzed using Editseq software (DNASstar Lasergene) (Burland, 2000). The homology of duIRF8 sequence with other known sequences was analyzed by NCBI BLAST program. The coding region sequences of IRF8 from other species (Table 2) were obtained from the NCBI website, and convert into text files using Editseq software. The phylogenetic relationship of IRF8 was established using the neighbor-joining algorithm in MEGA5.1 (Kumar et al., 2018), and GenBank accession numbers of the reference sequences used in the phylogenetic analysis are shown in Table 2. The partial gene sequences of IRF8 obtained in the current study were translated into protein sequences using the EditSeq program. The protein sequence was compared using Clustal X software (Thompson et al., 1997), edited using BOXSHADE, and finally the result of amino acid alignment was obtained.

### Quantitative Real Time PCR (qPCR)

QPCR analysis is used to study the tissue distribution and expression of duIRF8, and the level of duIRF8 changes in the brain and spleen after DTMUV, NDRV,

**Table 1.** Primer sequences used in this study.

Primer name	Nucleotide sequence (5'-3')	Purpose
duIRF8-F	GGGATGGACAGACAGACGTT	Gene cloning
duIRF8-R	GACTCCGGACTGAGAACAGC	
q-duIRF8-F	GATGTACGGACATGGACTG	qRT-PCR
q-duIRF8-R	CCTGAATGATGCTGCTCGTA	
q- $\beta$ -actin-F	GGTATCGGCAGCAGTCTTA	qRT-PCR
q- $\beta$ -actin-R	TTACACAGAGCGAGTAACCT	

Note: F: forward primer; R: reverse primer; q = qRT-PCR.

**Table 2.** Reference sequences information of IRF8.

Species	GeneBank accession numbers
<i>Alligator Sinensis</i>	XP_014374995.1_1
<i>Anser cygnoides</i>	XP_013056913.1_1
<i>Bos taurus</i>	XP_005218782.1_1
<i>Callorhinchus milii</i>	XP_007887425.1_1
<i>Cavia porcellus</i>	XP_003461072.1_1
<i>Chelonia mydas</i>	XP_027677578.2_1
<i>Homo</i>	NP_001350836.1_1
<i>Felis catus</i>	XP_023100909.1_1
<i>Leptonychotes</i>	XP_006743818.1_1
<i>Mus musculus</i>	NP_001288740.1_1
<i>Oreochromis niloticus</i>	XP_005467184.1_1
<i>Ovis aries</i>	XP_027833509.1_1
<i>Pelodiscus sinensis</i>	XP_006137424.1_1
<i>Sus scrofa</i>	XP_020949138.1_1
<i>Meleagris gallopavo</i>	XP_010716521.1_1

and DPV infection. 1.0  $\mu$ g of total RNA from 21 tissues was reverse transcribed into cDNA, and qPCR was performed using ChamQ SYBR qPCR Master Mix (Q311, Vazyme) in the 7500 Fast Real-Time PCR system (Applied Biosystems, Carlsbad, CA). QPCR was performed in a volume of 20  $\mu$ L, which contained 10  $\mu$ L 2  $\times$  SYBR Green Real Time PCR Master Mix, 0.4  $\mu$ M each of gene-specific forward and reverse primers (Table 1) and 1.0  $\mu$ L diluted cDNA (50 ng/ $\mu$ L) and 8.2  $\mu$ L ddH<sub>2</sub>O. The reaction conditions were predenaturation at 94°C for 5 min, followed by 40 cycles of denaturation at 94°C for 10 s, annealing at 60°C for 34 s, and  $\beta$ -actin is used as an endogenous control. The expression level of duIRF8 was normalized to  $\beta$ -actin, and further expressed as a fold change relative to the control expression level in the gene expression analysis after virus infection according to the  $2^{-\Delta\Delta C_t}$  method.

### Statistical Analysis

All values are represented as mean  $\pm$  SD of triplicate samples, and analyzed by using SPSS19.0 software and performed using graph prism 5.0 software. Students' *t*-test were used to analyze the difference between two groups. One-way ANOVA was used to analyze data with multiple groups.

## RESULTS

### Molecular Characterization of duIRF8

The duIRF8 ORF is 1293 nucleotides long and encodes a putative protein of 430 amino acids (GenBank: MZ960930). DuIRF8 is divided into 7 regions: N terminus, DNA-binding domain (DBD), nuclear localization signal (NLS), transactivation domain, exon 6, IRF-association domain (IAD) and C terminus. The multiple alignments revealed that the putative protein has 3 conserved domains: the N-terminal DBD domain, the C-terminal IAD domain and the NLS domain, which are marked in different ways in Figure 1.

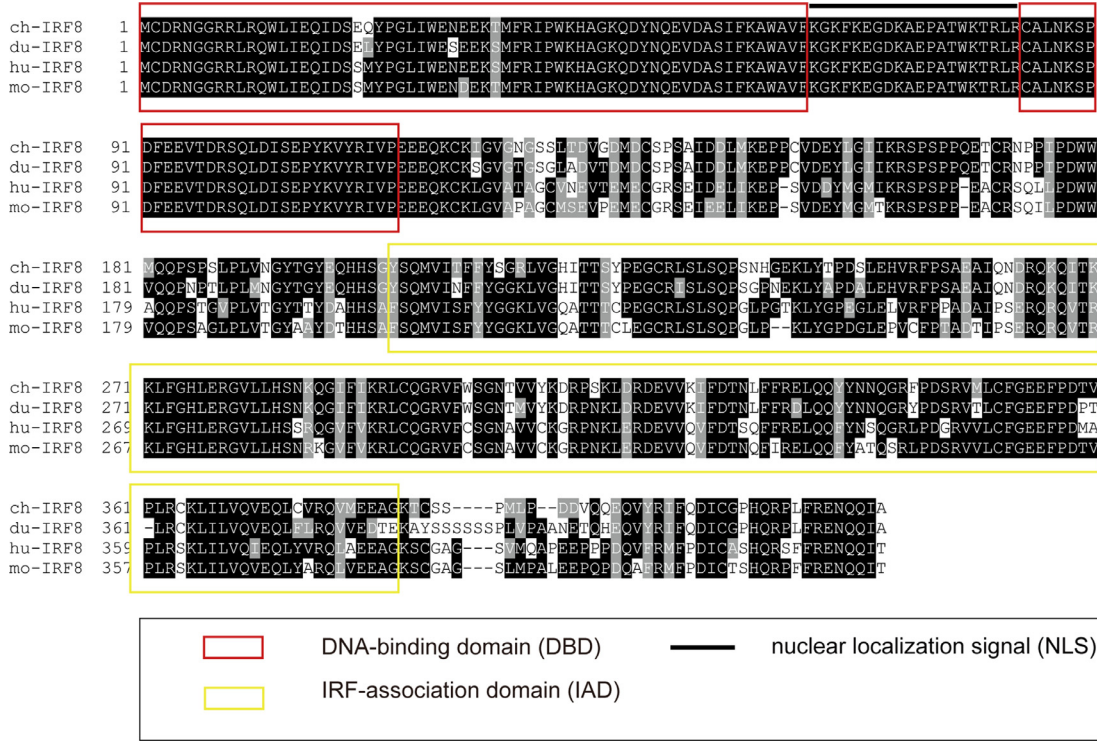


**Figure 1.** Alignment of the deduced AA sequence of duIRF8 with other animals. DuIRF8 can be divided into 7 regions: N terminus, DNA-binding domain, putative nuclear localization signal, transactivation domain, exon 6, IRF-association domain and C terminus. Figure 1 annotates the 3 conserved domains of the IRF8 protein sequence in different ways: the N-terminal DBD domain (the red box in Figure 1), the C-terminal IAD domain (the yellow box in Figure 1) and the NLS domain (the black line in Figure 1). Abbreviations: Ho, Homo sapiens; Mu, Mus musculus; Ch, Gallus gallus; Du, Cherry Valley Duck.

## Phylogenetic Analysis of duIRF8

In order to determine the phylogenetic position of duIRF8, the overall amino acid sequence of IRF8 from mammals, birds, amphibians, and fish was downloaded from NCBI to construct a phylogenetic tree (Figure 2A). The results show that the Cherry Valley duck has the highest homology with *Anser cygnoides*, with a homology of 96.5% (Figure 2B). Besides, the duIRF8 has very high sequence homology with *Meleagris gallopavo* and *Chelonia mydas*, but it is relatively distantly related to fish.

## Tissue Distribution of duIRF8 in Healthy Cherry Valley Duck

The tissue distribution of duIRF8 was examined by qPCR using the bursa of fabric as a reference tissue and  $\beta$ -actin gene as an internal reference in 21 tissue types including heart, liver, spleen, lung, kidney, brain, cerebellum, brainstem, thymus, pancreas, bursa of fabric, duodenum, jejunum, ileum, cecum, skin, muscle, glandular stomach, muscular stomach, trachea and esophagus of healthy Cherry Valley duck. The highest expression level in the liver is 154-fold that of the bursa of Fabricius, and the expression level in the heart and cecum is also very high, reaching about 100-fold, while the expression level is lower in muscle, skin, glandular stomach, and muscular stomach (Figure 3).

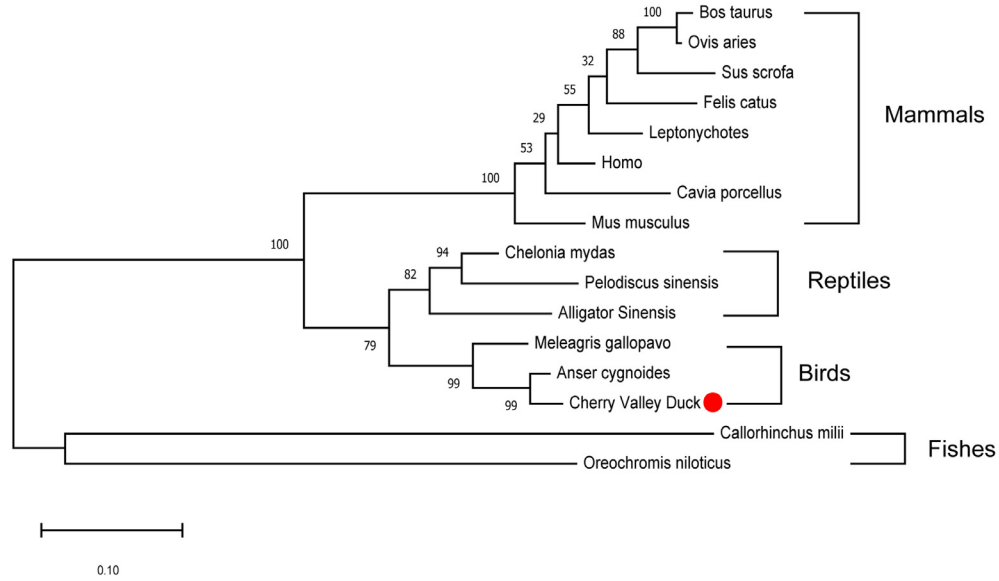
## Expression Profiles of duIRF8 in the Viral Infected Ducks

In order to further understand the role of duIRF8 in the antiviral immune response, qPCR was used to study its gene expression in two selected tissues (kidney and brain) of DTMUV, NDRV, and DPV challenged Cherry Valley ducks at 1, 3, 5 dpi. The expression of IRF8 in the spleen and brain of Cherry Valley ducks was up-regulated at 1, 3, 5 dpi after the 3 virus infections, and reached differences and significant levels. Upon challenge of DTMUV, duIRF8 was significantly induced in the spleen and brain with a peak transcript level at 3 dpi. The maximum induction of the spleen at 3 dpi was 342.2-fold ( $P < 0.01$ ) (Figure 4A) over control, and brain was 1385.9-fold ( $P < 0.01$ ) (Figure 4B). In the case of NDRV challenge, the expression of duIRF8 in the spleen (Figure 4C) is significantly higher than that in the brain (Figure 4D), and the expression level gradually decreases at 1, 3, 5 dpi. Upon challenge with DPV, duIRF8 expression was also up-regulated. DuIRF8 was markedly induced in the spleen (Figure 4E) and less induced in the brain (Figure 4F).

## DISCUSSION

Studies on the IRF family have shown that IRF has received great attention because of its important roles in regulating the expression of inflammatory cytokines, initiating antiviral responses, and controlling cell cycle and apoptosis (Au et al., 1998; Honda et al., 2005). IRF8 is

A



B

		Percent Identity																	
		1	2	3	4	5	6	7	8	9	10	11	12	13	14	15	16		
Divergence	1	■	83.0	70.9	54.1	70.7	87.0	72.4	70.0	72.6	72.5	56.2	71.2	83.4	70.9	82.8	81.6	1	Alligator Sinensis
	2	19.3	■	71.5	54.0	69.8	83.1	72.9	71.2	73.1	73.2	54.1	72.2	80.8	71.5	92.0	96.5	2	Anser cygnoides
	3	36.7	35.9	■	51.1	86.9	74.9	90.2	88.8	90.9	88.7	52.7	98.8	72.6	91.1	72.6	71.1	3	Bos taurus
	4	69.5	69.9	76.9	■	51.4	54.2	51.6	51.4	51.6	51.1	50.6	51.4	54.4	50.9	54.3	53.8	4	Callorhynchus mydas
	5	37.1	38.6	14.5	76.3	■	73.3	89.0	84.3	85.9	87.3	52.0	87.4	71.0	85.5	70.8	70.2	5	Cavia porcellus
	6	14.3	19.2	30.5	69.3	33.0	■	75.9	73.8	75.2	76.0	54.8	74.9	89.5	75.2	84.3	82.5	6	Chelonia mydas
	7	34.4	33.7	10.6	75.7	11.9	29.1	■	88.5	91.6	90.1	53.4	91.1	73.5	88.3	74.1	72.8	7	Homo sapiens
	8	38.3	36.3	12.2	76.3	17.7	32.3	12.5	■	91.3	86.1	52.2	89.0	71.7	87.6	71.9	71.4	8	Felis catus
	9	34.0	33.3	9.8	75.7	15.6	30.2	9.0	9.2	■	88.9	53.4	90.9	73.3	89.5	73.3	72.8	9	Leptonychotes
	10	34.3	33.1	12.3	76.9	14.0	29.0	10.6	15.4	12.0	■	53.2	88.7	73.4	85.9	74.2	72.6	10	Mus musculus
	11	64.6	69.6	72.9	78.2	74.7	67.9	71.1	74.1	71.1	71.7	■	53.0	54.1	52.2	55.0	54.4	11	Oreochromis
	12	36.3	34.8	1.2	76.3	13.9	30.5	9.5	11.9	9.8	12.3	72.3	■	72.1	91.6	73.1	71.8	12	Ovis aries
	13	18.8	22.3	34.1	68.8	36.7	11.3	32.7	35.6	33.0	32.9	69.7	34.8	■	71.9	82.2	80.4	13	Pelodiscus sinensis
	14	36.7	35.9	9.5	77.6	16.2	30.2	12.8	13.6	11.4	15.7	74.1	9.0	35.2	■	71.7	70.9	14	Sus scrofa
	15	19.6	8.5	34.0	69.0	37.0	17.7	31.9	35.2	32.9	31.7	67.5	33.3	20.4	35.5	■	91.1	15	Meleagris gallopavo
	16	21.1	3.6	36.4	70.2	38.0	20.0	33.8	36.1	33.8	34.0	68.8	35.3	22.8	36.8	9.5	■	16	Cherry Valley duck ●
		1	2	3	4	5	6	7	8	9	10	11	12	13	14	15	16		

**Figure 2.** Phylogenetic analysis and sequence similarity of IRF8. The duIRF8 is marked with a red dot in Figure 2, and the homology with other animal IRF8 sequences is shown by the phylogenetic tree. Download the coding region sequence of IRF8 of other animals from the NCBI website, use Editseq software to convert it into a text file, and use the neighbor-joining algorithm in MEGA5.1 to construct the phylogenetic tree. The accession numbers of the sequences used in Genbank are shown in Table 2. The animals involved include mammals, birds, reptiles, and fish.

mainly expressed in cells of the immune system, such as bone marrow cells and lymphocytes (Lu, 2008), and is necessary for the development and maturation of bone marrow cells, such as dendritic cells and macrophages, and for the expression of immune functions such as antigen processing and presentation.

In this study, duIRF8 was cloned for the first time and its structure was analyzed. The duIRF8 cDNA contains a 1293 bp open reading frame (ORF) that encodes 430 AA. The duIRF8 protein is composed of 3 major domains found in all known IRF8s: an N-terminal DBD domain, a NLS domain and a C-terminal IAD domain. The DBD of IRFs has extensive homology and can form a helix-turn-helix domain that recognizes and binds to a

consensus DNA sequence. DBD is located on a variety of immune or immune-related gene promoters, which is characterized by a series of 5 highly conserved tryptophan-rich repeats (Tamura et al., 2008). When the virus invades, IRF8 in the body activates the expression of immune-related genes through the DBD domain, thereby exerting an antiviral immune response. The IAD domain is also a conserved domain in IRFs, which participates in the interaction with other members of the IRF family, other transcription factors and cofactors to give each IRF specificity (Chen and Royer, 2010). There is also a conserved domain, NLS, which is located in DBD, but its specific mechanism of action has not yet been studied clearly. The homology comparison between

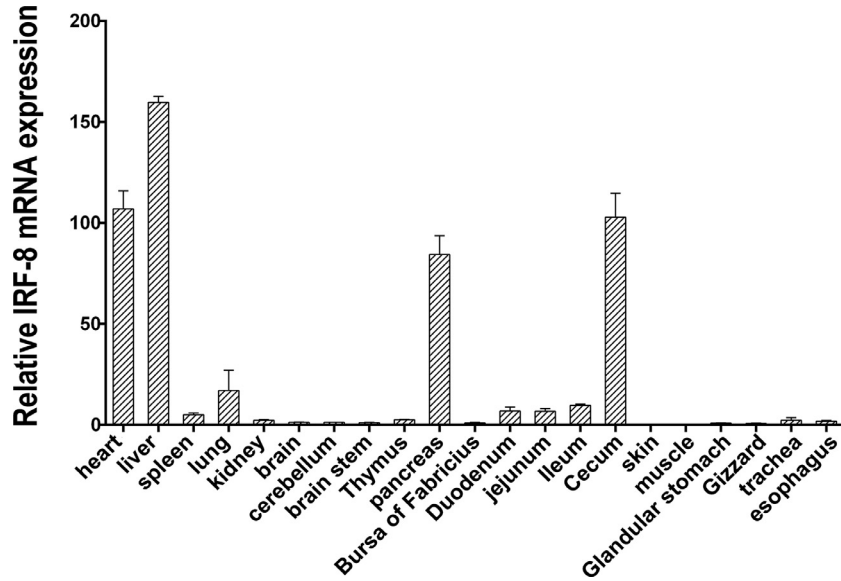


**Figure 3.** Tissue distribution of duIRF8 transcripts in healthy Cherry Valley duck. The expression of IRF8 mRNA in various tissues of healthy Cherry Valley ducks was detected by qRT-PCR. The obtained mean uses  $\beta$ -actin gene as internal reference and heart as reference tissue. The quantification of the relative expression level of the target gene and the reference gene  $\beta$ -actin is calculated by the  $2^{-\Delta\Delta Ct}$  method. All samples are set to 3 replicates to ensure the accuracy of the experiment.

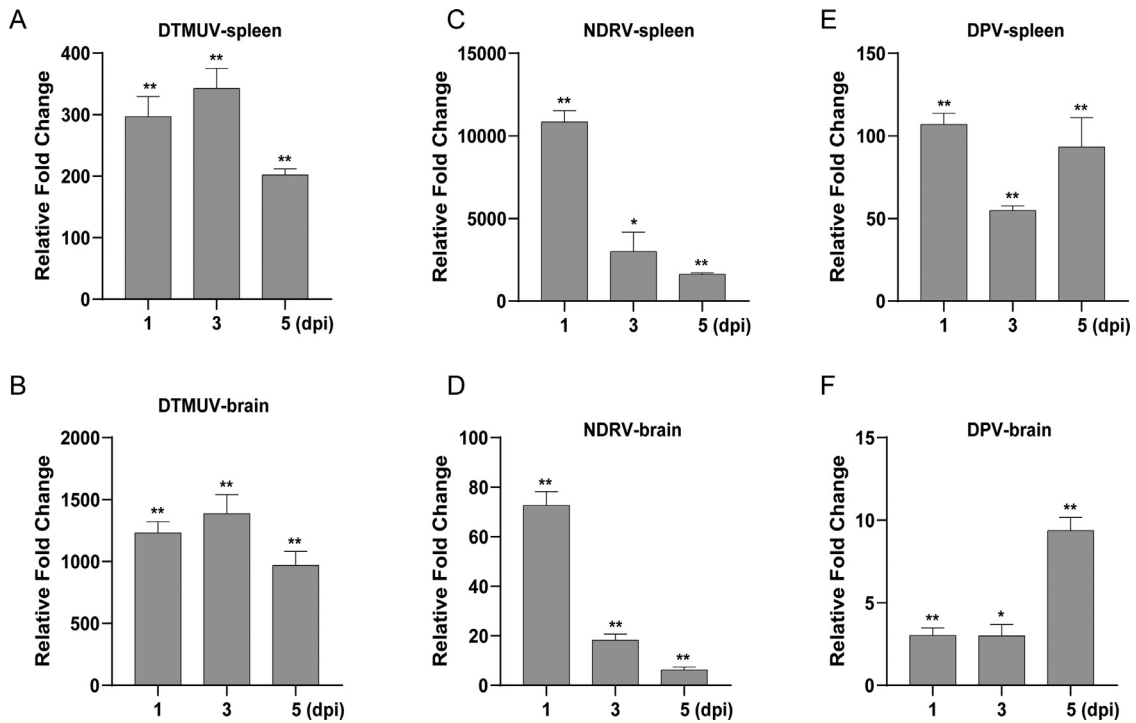


**Figure 4.** Analysis of duIRF8 transcript after infection with the 3 viruses (A) DTMUV-spleen, (B) DTMUV-brain, (C) NDRV-spleen, (D) NDRV-brain, (E) DPV-spleen, and (F) DPV-brain. The relative expression levels were calculated with the  $2^{-\Delta\Delta Ct}$  method. The data of each group are expressed as mean  $\pm$  SD, and the students'  $t$  test is used to analyze the difference between the two groups of data. In the figure, “\*” indicates that the statistical value of  $P < 0.05$  is considered to be significant, and “\*\*” indicates that the statistical value of  $P < 0.01$  is considered to be extremely significant.

duIRF8 and IRF8 of mammals, poultry, fish, and amphibians was carried out, and a phylogenetic tree was constructed. The phylogenetic tree shows that duIRF8 is most closely related to the IRF8 sequence in *Anser cygnoides* followed by those in *Meleagris gallopavo*. In addition, duIRF8 shares 72.8% sequence identity with *Homo sapiens* and 53.8% identity with *Callorhinchus mydas*. This fact suggests that duIRF8 has a close relationship with other birds. Results of qPCR analysis

showed that duIRF8 transcripts can be detected in all healthy Cherry Valley duck tissues examined. DuIRF8 has the highest expression in the liver, followed by the heart and cecum, while the expression in skin, muscle, and other tissues is low. The liver has the functions of immune defense, hematopoiesis, and detoxification. DuIRF8 has the highest expression in the liver, indicating that duIRF8 plays an important role in hematopoiesis and immune system.

Previous studies have shown that DTMUV, NDRV, and DPV can infect Cherry Valley ducks and cause obvious immune responses (Li et al., 2016a,c; Lv et al., 2019). Since DTMUV, NDRV and DPV all cause neurological and digestive symptoms, we choose the spleen and brain as targets to detect changes in duIRF8 expression. In this study, we investigate whether duIRF8 is involved in this process with stimulation of DTMUV, NDRV and DPV by a gene expression analysis. The results showed that in the early stage of virus infection, the expression of duIRF8 in the spleen and brain was enhanced by DTMUV, NDRV and DPV. Besides, our study showed that in DTMUV challenge case, duIRF8 is significantly induced in both the brain and spleen, but the degree of induction is significantly higher in the brain than in the spleen. It is worth mentioning that duIRF8 reached the highest induction at 3 dpi in both the brain and spleen, which indicate that duIRF8 may participate in the early anti-DTMUV infection immunity in the spleen and brain. Different from DTMUV, when NDRV is infected, the expression level of duIRF8 in the spleen is much higher than that in the brain, and the expression level of duIRF8 in both decreases gradually at 1, 3 and 5 dpi, indicating that duIRF8 in the spleen and brain participate in the initial anti-NDRV immunization. The spleen exhibited the high and early increase for duIRF8, suggesting the important immune function of spleen duIRF8 in the body's early anti-NDRV infection. Compared with DTMUV and NDRV infection, the level of duIRF8 induced by DPV infection is greatly reduced, which indicates that the induction of duIRF8 by DPV is not as strong as that of DTMUV and NDRV. Collectively, after ducks are infected with the virus, IRF8 in the spleen and brain is induced to varying degrees, which means that duIRF8 participates in the antiviral innate immunity of the Cherry Valley duck's immune organs and nervous system, and may play a key role in it. This is consistent with the study of IRF8 on mammals. Studies on IRF8 knockout mice have shown that the lack of IRF8 affects the expression of mouse microglia and macrophage activation genes, thereby enhancing the replication of Japanese viral encephalitis in the mouse brain (Tripathi et al., 2021). At the same time, the spleen showed the earliest and most IRF8 increase after virus infection, indicating the importance of immunity.

In summary, the structural and expression characteristics of duIRF8 in Cherry Valley duck were reported in the present study. Besides, we found that duIRF8 is significantly induced in the spleen and brain in the early stages of DTMUV, NDRV and DPV infection, which proves that duIRF8 is involved in the antiviral immunity of Cherry Valley ducks. Our findings may help a further understanding of the functions and evolution of duIRF8. Our research on duIRF8 is only preliminary, and further research remains to be done to explain the mechanism of duIRF8 in the antiviral process and its influence on upstream and downstream cytokines.

## ACKNOWLEDGMENTS

This work was supported by the National Natural Science Foundation of China (31972664), the China Postdoctoral Science Foundation (2018M632268 and 2019T120404) and the Local Science and Technology Development Fund Project Guided by the Central Government of Shandong Province (YDZX20203700004857).

Author Contributions: Tingting Zhang and Xinyu Zhai wrote the manuscript and performed the most of the experiments. Tianqi Hong and Tianxu Li provided help for the experiment and writing, Jinchao Wang and Bin Xing helped complete the animal experiment, Xiuyuan Wang and Runchun Miao collected samples. Liangmeng Wei designed the study and polished the article.

Ethics Statement: This animal study was reviewed and approved by Shandong Agricultural University Animal Care and Use Committee (no. SDAUA-2017-045).

## DISCLOSURES

The authors declare that the research was conducted in the absence of any commercial or financial relationships that could be construed as a potential conflict of interest.

## REFERENCES

- Au, W. C., P. A. Moore, D. W. LaFleur, B. Tombal, and P. M. Pitha. 1998. Characterization of the interferon regulatory factor-7 and its potential role in the transcription activation of interferon A genes. *J. Biol. Chem.* 273:29210–29217.
- Burgess, E. C., and T. M. Yuill. 1981. Vertical transmission of duck plague virus (DPV) by apparently healthy DPV carrier waterfowl. *Avian Dis.* 25:795–800.
- Burland, T. G. 2000. DNASTAR's Lasergene sequence analysis software. *Methods Mol. Biol.* 132:71–91.
- Chen, S.-Y., S.-L. Chen, F.-Q. Lin, S. Wang, B. Jiang, X.-X. Cheng, X.-L. Zhu, and Z.-L. Li. 2012a. The isolation and identification of novel duck reovirus. *Bing du xue bao = Chin. J. Virol.* 28:224–230.
- Chen, W., and W. E. Royer Jr. 2010. Structural insights into interferon regulatory factor activation. *Cell. Signal.* 22:883–887.
- Chen, Z., Y. Zhu, C. Li, and G. Liu. 2012b. Outbreak-associated Novel Duck Reovirus, China, 2011. *Emerg. Infect. Dis.* 18:1209–1211.
- Chmielewski, S., A. Piaszyk-Borychowska, J. Wesoly, and H. A. R. Bluysen. 2016. STAT1 and IRF8 in vascular inflammation and cardiovascular disease: diagnostic and therapeutic potential. *Int. Rev. Immunol.* 35:434–454.
- Eisenbeis, C. F., H. Singh, and U. Storb. 1995. Pip, a novel IRF family member, is a lymphoid-specific, PU.1-dependent transcriptional activator. *Genes Dev.* 9:1377–1387.
- Hansen, W. R., S. E. Brown, S. W. Nashold, and D. L. Knudson. 1999. Identification of duck plague virus by polymerase chain reaction. *Avian Dis.* 43:106–115.
- Honda, K., H. Yanai, H. Negishi, M. Asagiri, M. Sato, T. Mizutani, N. Shimada, Y. Ohba, A. Takaoka, N. Yoshida, and T. Taniguchi. 2005. IRF-7 is the master regulator of type-I interferon-dependent immune responses. *Nature* 434:772–777.
- Kumar, S., G. Stecher, M. Li, C. Knyaz, and K. Tamura. 2018. MEGA X: molecular evolutionary genetics analysis across computing platforms. *Mol. Biol. Evol.* 35:1547–1549.
- Li, Z., Y. Cai, G. Liang, S. El-Ashram, M. Mei, W. Huang, X. Li, W. Li, C. He, and S. Huang. 2018. Detection of Novel duck

- reovirus (NDRV) using visual reverse transcription loop-mediated isothermal amplification (RT-LAMP). *Sci. Rep.* 8:14039.
- Li, N., T. Hong, R. Li, M. Guo, Y. Wang, J. Zhang, J. Liu, Y. Cai, S. Liu, T. Chai, and L. Wei. 2016a. Pathogenicity of duck plague and innate immune responses of the Cherry Valley ducks to duck plague virus. *Sci. Rep.* 6:32183.
- Li, N., T. Hong, R. Li, Y. Wang, M. Guo, Z. Cao, Y. Cai, S. Liu, T. Chai, and L. Wei. 2016b. Cherry Valley ducks mitochondrial antiviral-signalling protein-mediated signaling pathway and antiviral activity research. *Front. Immunol.* 7:377.
- Li, N., T. Hong, Y. Wang, Y. Wang, K. Yu, Y. Cai, S. Liu, L. Wei, and T. Chai. 2016c. The pathogenicity of novel duck reovirus in Cherry Valley ducks. *Vet. Microbiol.* 192:181–185.
- Lu, R. 2008. Interferon regulatory factor 4 and 8 in B-cell development. *Trends Immunol.* 29:487–492.
- Lv, C., R. Li, X. Liu, N. Li, and S. Liu. 2019. Pathogenicity comparison of duck Tembusu virus in different aged Cherry Valley breeding ducks. *BMC Vet. Res.* 15:282.
- Miyamoto, M., T. Fujita, Y. Kimura, M. Maruyama, H. Harada, Y. Sudo, T. Miyata, and T. Taniguchi. 1988. Regulated expression of a gene encoding a nuclear factor, IRF-1, that specifically binds to IFN-beta gene regulatory elements. *Cell* 54:903–913.
- Nehyba, J., R. Hrdlickova, J. Burnside, and H. R. Bose Jr. 2002. A novel interferon regulatory factor (IRF), IRF-10, has a unique role in immune defense and is induced by the v-Rel oncoprotein. *Mol. Cell. Biol.* 22:3942–3957.
- Nice, T. J., M. T. Baldrige, B. T. McCune, J. M. Norman, H. M. Lazear, M. Artyomov, M. S. Diamond, and H. W. Virgin. 2015. Interferon-lambda cures persistent murine norovirus infection in the absence of adaptive immunity. *Science* 347:269–273.
- Park, H., Z. Li, X. O. Yang, S. H. Chang, R. Nurieva, Y.-H. Wang, Y. Wang, L. Hood, Z. Zhu, Q. Tian, and C. Dong. 2005. A distinct lineage of CD4 T cells regulates tissue inflammation by producing interleukin 17. *Nat. Immunol.* 6:1133–1141.
- Pathak, S., S. Ma, V. Shukla, and R. Lu. 2013. A role for IRF8 in B cell anergy. *J. Immunol.* 191:6222–6230.
- Pestka, S., C. D. Krause, D. Sarkar, M. R. Walter, Y. Shi, and P. B. Fisher. 2004. Interleukin-10 and related cytokines and receptors. *Annu. Rev. Immunol.* 22:929–979.
- Slifka, M. K., and J. L. Whitton. 2000. Antigen-specific regulation of T cell-mediated cytokine production. *Immunity* 12:451–457.
- Tamura, T., H. Yanai, D. Savitsky, and T. Taniguchi. 2008. The IRF family transcription factors in immunity and oncogenesis. *Annu. Rev. Immunol.* 26:535–584.
- Tang, Y., Y. Diao, X. Gao, C. Yu, L. Chen, and D. Zhang. 2012. Analysis of the complete genome of Tembusu virus, a flavivirus isolated from ducks in China. *Transboundary Emerg. Dis.* 59:336–343.
- Thompson, J. D., T. J. Gibson, F. Plewniak, F. Jeanmougin, and D. G. Higgins. 1997. The CLUSTAL\_X windows interface: flexible strategies for multiple sequence alignment aided by quality analysis tools. *Nucleic Acids Res.* 25:4876–4882.
- Tripathi, A., B. S. Rawat, S. Addya, M. Surjit, P. Tailor, S. Vrati, and A. Banerjee. 2021. Lack of interferon (IFN) regulatory factor 8 associated with restricted IFN-gamma response augmented Japanese encephalitis virus replication in the mouse brain. *J. Virol.* 95:e00406-21.
- Twum, D. Y. F., S. H. Colligan, N. C. Hoffend, E. Katsuta, E. C. Gomez, M. L. Hensen, M. Seshadri, M. J. Nemeth, and S. I. Abrams. 2019. IFN regulatory factor-8 expression in macrophages governs an antimetastatic program. *JCI Insight* 4:e124267.
- Weaver, C. T., R. D. Hatton, P. R. Mangan, and L. E. Harrington. 2007. IL-17 family cytokines and the expanding diversity of effector T cell lineages. *Annu. Rev. Immunol.* 25:821–852.
- Yan, L. P., P. X. Yan, J. W. Zhou, Q. Y. Teng, and Z. J. Li. 2011a. Establishing a TaqMan-Based Real-Time PCR Assay for the rapid detection and quantification of the newly emerged duck tembusu virus. *Virol. J.* 8:464.
- Yan, P., Y. Zhao, X. Zhang, D. Xu, X. Dai, Q. Teng, L. Yan, J. Zhou, X. Ji, S. Zhang, G. Liu, Y. Zhou, Y. Kawaoka, G. Tong, and Z. Li. 2011b. An infectious disease of ducks caused by a newly emerged Tembusu virus strain in mainland China. *Virology* 417:1–8.
- Yanai, H., H. Negishi, and T. Taniguchi. 2012. The IRF family of transcription factors Inception, impact and implications in oncogenesis. *Oncoimmunology* 1:1376–1386.
- Yu, K. X., Z. Z. Sheng, B. Huang, X. L. Ma, Y. F. Li, X. Y. Yuan, Z. M. Qin, D. Wang, S. Chakravarty, F. Li, M. X. Song, and H. C. Sun. 2013. Structural, antigenic, and evolutionary characterizations of the envelope protein of newly emerging Duck Tembusu Virus. *PLoS One* 8:e71319.
- Yun, T., W. C. Ye, Z. Ni, D. B. Zhang, and C. Zhang. 2012. Identification and molecular characterization of a novel flavivirus isolated from Pekin ducklings in China. *Vet. Microbiol.* 157:311–319.